

Effects of stimulated emission on radiative transfer with partial redistribution

K.E. Rangarajan, D. Mohan Rao, and A. Peraiah

Indian Institute of Astrophysics, Bangalore 560 034, India

Received March 17, 1989; accepted January 27, 1990

Abstract. We study the non-LTE line transfer with stimulated emission in this paper. Stimulated emission is important for red transitions in hot stars and infrared transitions in cool stars. We investigate the deviation of the absorption and emission profiles from each other for a two-level atomic model with the line scattering described by the angle-averaged redistribution functions. The partial redistribution formalism has been used while solving the radiative transfer equation. The correct expression for the source function derived by Baschek, Mihalas and Oxenius (1981) has been employed to obtain the emission profile and the radiation field. From this study, we get the following results: The redistribution function R_{III} gives the emission profile same as that of the absorption profile (like complete redistribution, CRD) in the core and also in the wings but with a small enhancement at the intermediate frequency points whether stimulated emission is present or not. The emergent emission profile is different from the absorption profile by several factors in the wings for R_{II} . When stimulated emission is present, we find the ratio of the emission profile to the absorption profile and also the intensity in the wings of the spectral lines to be reduced for R_{II} .

Key words: lines: formation – lines: profile – radiation transfer

1. Introduction

The emission profile ψ_ν is defined as the fraction of all atoms in the upper state which, if they decay radiatively, emit photons of frequency ν as seen in the laboratory frame (Mihalas, 1978). In general, the absorption and emission profiles depend on the radiation field as well as on the velocity distribution of atoms in the lower and upper states. When stimulated emission is present, the velocity distribution function of nonexcited atoms $F_1(v)$ cannot be specified a priori and so we find the absorption profile ϕ_ν is dependent on the radiation field. Therefore it has to be determined self-consistently together with the radiation field (Oxenius, 1986). This requires complex iteration process. For most of the resonance lines formed in stellar atmospheres, we can assume that the ground state is populated naturally (i.e. infinitely sharp ground state). If we further approximate the distribution function $F_1(v)$ to be Maxwellian, then the absorption profile function ϕ_ν is specified. In all our calculations presented in this study, we have made the above assumptions.

The scattering of photons in spectral line formation studies can be assumed to be either strictly coherent or completely redistributed over the line profile in the laboratory frame. Neither of these extreme conditions is achieved in stellar atmospheres. Therefore it is necessary to consider the redistribution of photons in angle and frequency which describes the scattering process precisely. This is known as the partial redistribution (PRD) formalism. If absorption and emission can be regarded as two independent processes, i.e., the assumption of complete redistribution, the equality of the absorption and emission profiles is assured. If there is any correlation between absorption and subsequent emission, we see that the emission profile is dependent on the radiation field. Since such a correlation exists in the partial frequency redistribution formalism, we find that the absorption and emission profiles need not be identical. Our aim is to find the deviation between the absorption and emission profiles when stimulated emission is important and the scattering process is described by the partial redistribution functions in radiative transfer calculations.

In the process of resonance scattering, an atom is excited from one bound state to another by the absorption of a photon, and then decays radiatively back to the original state, with the emission of a photon. Different laboratory frame redistribution (LFR) functions exist for describing the line scattering under different conditions. They are denoted as R_I , R_{II} and R_{III} in Hummer's (1962) notation. The LFRs are obtained by folding the atomic frame redistribution functions with the velocity distribution of the atoms which is usually taken to be a Maxwellian. The R_I redistribution describes the scattering process when both the atomic states are infinitely sharp. In this case, the atomic frame scattering is purely coherent. A resonance line formed with a sharp lower state and an upper state broadened by natural damping is described by the redistribution function R_{II} . Hence in the *atom's frame*, the scattering is coherent and the absorption profile is Lorentzian. R_{III} describes the frequency redistribution of a line having a sharp lower state but the upper state radiatively and collisionally broadened. Hence in the atom's frame there is complete frequency redistribution with a Lorentzian absorption profile. We find the R_{II} (LFR) function to be coherent in the wings and the R_{III} function to be non-coherent. Therefore they represent two different types of scattering mechanisms.

Oxenius (1965) gave some expressions for calculating the emission profile and also discussed certain idealized cases where the absorption and emission profiles become equal. The sub-state formalism of Milkey and Mihalas (1973) allows a quantitative study but requires elaborate calculations involving the iteration

Send offprint requests to: K.E. Rangarajan

of the solution of linearized equations to calculate the emission profile even for a two-level atomic model. Their method follows the multi-level atom approach to solve for the emission profile. Heasley and Kneer (1976) applied a slight variation of the sub-state formalism of Milkey and Mihalas (1976) to the problem of the formation of Hydrogen Ly- α and Ca II K line in the solar chromosphere. Steinitz and Shine (1973) investigated the assumption of the equality of the absorption and emission profiles and gave quantitative results for a two-level atom model with the scattering described by the R_I redistribution. They have used parametrized models to describe their problem. Baschek et al. (1981) showed that the formulation given by Mihalas (1978) of the stimulated emission term is incorrect. They gave correct expressions for the statistical equilibrium equations incorporating the angle-averaged redistribution functions. Hubeny (1981) extended the Oxenius' two-level treatment for the multi-level atoms and derived a generalized emission profile.

We note that the expressions given by Baschek et al. are consistent with the equations of Steinitz and Shine (1973). Moreover, we find that the expressions obtained by Oxenius (1986) reduce to the equations of Steinitz and Shine under the approximations mentioned in the first paragraph of this paper. Therefore we will closely follow the formalism of Steinitz and Shine in our present study. We have obtained the emission profile when stimulated emission is not negligible. We have studied the effect of the angle-averaged redistribution functions R_{II} and R_{III} on line formation and the emission profile. In Sect. 2, the frequency dependent source function and the method of solution are described. We study only parametrized models so that we can understand the underlying physical processes and the effect of different assumptions usually made in the spectral line formation calculations. In Sect. 3, we discuss the results. We illustrate in graphical form the ratio of the emission profile to the absorption profile for various cases. In Sect. 4, the main conclusions are briefly summarized.

2. The source function including the emission profile

The transfer equation for a two-level atom in plane-parallel geometry without continuous absorption can be written as

$$\mu \frac{dI_\nu}{d\tau_\nu} = \phi_\nu (I_\nu - S_\nu), \quad (1)$$

where I_ν is the specific intensity of the ray making an angle $\cos^{-1}\mu$ with the axis of symmetry and S_ν is

$$S_\nu = \frac{(2h\nu^3/c^2)(g_1 n_2 \psi_\nu / g_2 n_1 \phi_\nu)}{1 - (g_1 n_2 \psi_\nu / g_2 n_1 \phi_\nu)}, \quad (2)$$

ψ_ν , ϕ_ν being the emission and absorption profiles, n_1 , n_2 are the number densities of the lower and upper levels respectively, c is the velocity of light, ν is the frequency, g_1 and g_2 are the statistical weights of the lower and upper levels. The statistical equilibrium equations for a two-level atom are (Baschek et al., 1981)

$$\begin{aligned} n_2 \psi_\nu \left(A_{21} + B_{21} \int J_{\nu'} \psi_{\nu'} d\nu' + C_{21} \right) \\ = n_1 \left(B_{12} \int J_{\nu'} R(\nu', \nu) d\nu' + C_{12} \psi_\nu^* \right). \end{aligned} \quad (3)$$

and

$$n_1 + n_2 = N_{\text{atom}}. \quad (4)$$

The angle-averaged redistribution and isotropic emission profile are used in deriving the above equation. The fact that the spontaneous and stimulated emission profiles are the same also enters into the derivation of Eq. (4) (Dirac, 1958). A_{21} , B_{21} , and B_{12} are the Einstein spontaneous emission, induced emission, and absorption coefficients, respectively. The first term in Eq. (3) represents the number of atoms which emit spontaneously. The integral in the second term accounts for all atoms which can be depleted by induced emission over all frequencies. C_{21} and C_{12} are the collisional de-excitation and excitation rates, respectively. The first term on the R.H.S. of Eq. (3) gives the number of atoms which absorb at frequency ν' and emit at frequency ν , summed over all ν' . Even though the notation ψ denotes the emission profile, here, the quantity ψ_ν^* is the natural excitation profile which is the same as the absorption profile ϕ_ν . Equation (4) represents the conservation of atoms and the total number of atoms, N_{atom} , is kept constant. Using Eqs. (2) and (3), Baschek et al. (1981) showed that the source function S_ν can be written as

$$S_\nu = \xi_\nu [J_R / \phi_\nu + \varepsilon' B], \quad (5)$$

where

$$\xi_\nu = [1 + (B_{21}/A_{21})(J_e - \omega_\nu J_a) + (C_{21}/A_{21})(1 - \omega_\nu e^{-h\nu/kT})]^{-1}, \quad (6)$$

with

$$\int J_{\nu'} \psi_{\nu'} d\nu' = J_e; \quad \int J_{\nu'} R(\nu', \nu) d\nu' = J_R,$$

and

$$\int J_{\nu'} \phi_{\nu'} d\nu' = J_a. \quad (7)$$

Equation (5) for the source function is equivalent to the expression used by Steinitz and Shine (1973) and can be written as

$$S_\nu = \frac{J_R / \phi_\nu + \varepsilon' B}{1 + \varepsilon' + \rho(E(\nu)/B)}, \quad (8)$$

where

$$\rho = \frac{B}{\sigma} = (e^{h\nu/kT} - 1)^{-1}; \quad \sigma = \frac{2h\nu^3}{c^2}; \quad (9)$$

$$E(\nu) = \omega_\nu \int J_{\nu'} \phi_{\nu'} \left(\frac{\omega_{\nu'}}{\omega_\nu} - 1 \right) d\nu' + \varepsilon' B (1 - \omega_\nu), \quad (10)$$

and

$$\omega_\nu = \frac{\psi_\nu}{\phi_\nu}; \quad \psi_\nu = \frac{\varepsilon' B \phi_\nu + J_R}{\varepsilon' B + J_e}, \quad \varepsilon' = \frac{C_{21}}{A_{21}} (1 - e^{-h\nu/kT}). \quad (11)$$

The $E(\nu)$ term renders the source function non-linear in the radiation field. The source function (Eq. 8) contains a thermal source term $\varepsilon' B$ which represents the photons that are created by collisional excitation, followed by radiative de-excitation. The term ε' in the denominator is a sink term that represents those photons that are destroyed by a collisional de-excitation following a photoexcitation. These two terms describe completely the coupling of the radiation field to the local thermal state of the gas. The scattering term may be viewed as the reservoir term that

represents the end result of the cumulative contributions of the source and sink terms over the entire interaction region.

2.1. Definition of optical depth

The optical depth for a medium consisting of two-level atoms is given by,

$$d\tau_v = -\frac{h\nu_0}{4\pi} (n_1 B_{12} \phi_v - n_2 B_{21} \psi_v) dz. \quad (12)$$

Defining

$$j_a = \frac{J_a}{B}, \quad j_e = \frac{J_e}{B}, \quad j_R = \frac{J_R}{B}, \quad (13)$$

and using Eq. (3) we obtain,

$$d\tau_v = \Delta\tau_v \left[1 - \frac{\rho(j_a + \varepsilon')\omega_v}{1 + \rho j_e + \varepsilon'(1 + \rho)} \right], \quad (14)$$

where

$$\Delta\tau_v = -\frac{h\nu_0}{4\pi} n_1 B_{12} \phi_v \Delta z. \quad (15)$$

The correction to the optical depth scale due to induced emission has to be taken into account for a self-consistent determination of the radiation field.

2.2. Procedure adopted for solving the transfer equation

We do not know J_e a priori. We therefore employ an iteration procedure to obtain the emission profile and the radiation field consistently. Initially, the transfer equation is solved by ignoring the $E(\nu)$ term in the source function and setting $d\tau(\nu) = \Delta\tau(\nu)$, for a given total optical depth T . To do this, we modified Peraiah's (1978) code which uses the discrete space theory of Grant and Hunt (1969). Knowing the radiation field, we obtain ψ_v , J_e , J_a and J_R . A new optical depth scale can be constructed from Eq. (14). Now we use Eq. (8) for the source function. With these definitions for the source function and optical depth scale, we solve the transfer equation once again to determine the new emission profile and the radiation field. This iteration procedure is continued till we reach 1% agreement for the emission profile and the radiation field between any two successive iteration values. It takes normally 5 iterations for $\rho = 2.0$.

We see that the parameter ρ measures the importance of stimulated emission. We have used the values 2.0 and 0.0 for ρ . ε' is assumed to be 10^{-3} or 10^{-4} . This fixes the contribution from the thermal sources. When ρ is very high, i.e., when the stimulated emission term is dominant, the procedure outlined above is unsuitable for solving the problem. The linearization technique given by Milkey and Mihalas (1973) is probably more appropriate in these situations.

We discretize the scattering integral over frequency and angle in the transfer equation by choosing 16 frequency points and two angles. The frequency grid is chosen as $x = [0, 5]$, where $x = (\nu - \nu_0)/\Delta\nu_D$, and $\Delta\nu_D$ is the Doppler width. The trapezoidal quadrature points are employed in the frequency grid and the Gauss-Legendre quadrature roots and weights are chosen for the angles in the interval (0, 1) (Abramowitz and Stegun, 1974). Since the problem gives a symmetric solution with respect to the line centre, only one half of the frequency grid is chosen. The Voigt

profile function with the damping parameter $a = 2.10^{-3}$ is employed.

3. Results and discussion

In Fig. 1, we have plotted $\log(R_{II}(x', x)/\phi(x')\phi(x))$. From this figure we find that the ratio is very much different from 1 especially in the wings. The function $\phi(x')\phi(x)$ is used in the CRD source function and we see that it differs from the redistribution functions by several orders of magnitude. Since the definition of the emission profile includes the redistribution function, we can expect the ratio $\psi(x)/\phi(x)$ to differ from 1 in the wings when it is used in the transfer calculations. This is what we find, and those results are discussed. In Fig. 2, we show $\log(R_{III}(x', x)/\phi(x')\phi(x))$ for $a = 2.10^{-3}$. This ratio $R_{III}(x', x)/\phi(x')\phi(x)$, remains close to 1 in the core and in the wings, but differs significantly from 1 at the intermediate frequencies. Therefore the emission profile $\psi(x)$ may not be different from the absorption profile $\phi(x)$ in the core and in the wings, but may

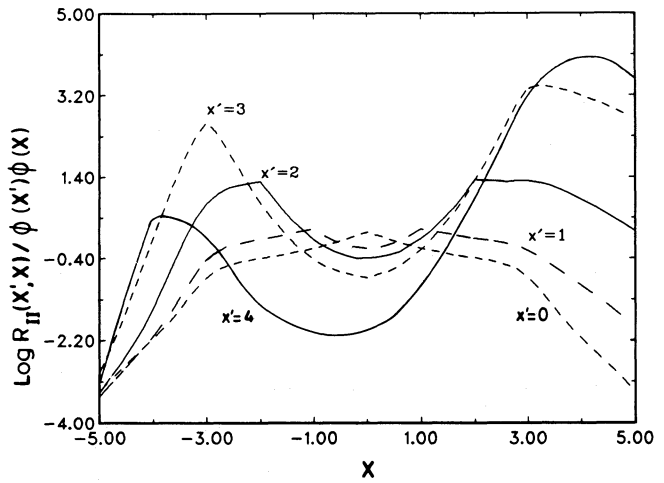


Fig. 1. Ratio of the redistribution function, $R_{II}(x', x)$, to the limiting case of complete noncoherence in the laboratory frame, $\phi(x')\phi(x)$. The absorption profile ϕ is a Voigt profile with $a = 2.10^{-3}$

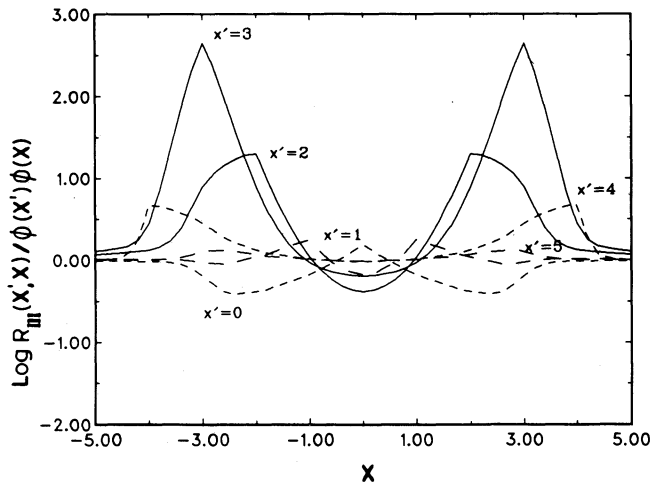


Fig. 2. Same as in Fig. 1 but for the R_{III} redistribution function

differ at the intermediate points. Our results confirm this prediction as shown below.

Cases considered

We have considered isothermal media with two different values for the optical thickness: One is an effectively thin medium with the total optical thickness at the line centre being $T=10^2$, and the other is an effectively thick medium with $T=10^5$. When $\epsilon' T \ll 1$ for a medium, it is considered as effectively thin, and when $\epsilon' T \gg 1$, it is classified as effectively thick. The thermal contribution parameter ϵ' has been chosen as either 10^{-3} or 10^{-4} . The R_{II} and R_{III} redistribution functions are used in the radiative transfer calculations. Two types of boundary conditions are chosen:

$$1) I(\tau=\tau_{\max}, \mu, x)=1; \quad I(\tau=0, -\mu, x)=0. \quad (16)$$

$$2) I(\tau=\tau_{\max}, \mu, x)=I(\tau=0, -\mu, x)=0. \quad (17)$$

The Planck function B is set equal to 1 in all cases.

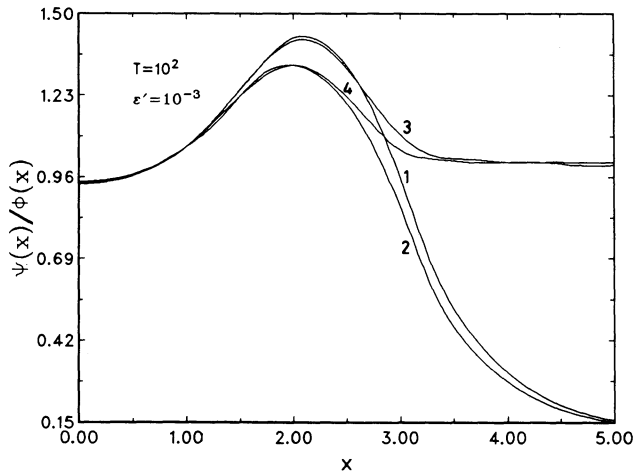


Fig. 3. Ratio of the emergent emission profile to the absorption profile for a self-emitting slab. In all the figures, symbols 1 and 2 denote the results for the R_{II} redistribution with stimulated emission parameter $\rho=0$ and 2, respectively. Corresponding results for the R_{III} redistribution are denoted by 3 and 4. The total optical depth of the medium is $T=10^2$, and $\epsilon'=10^{-3}$

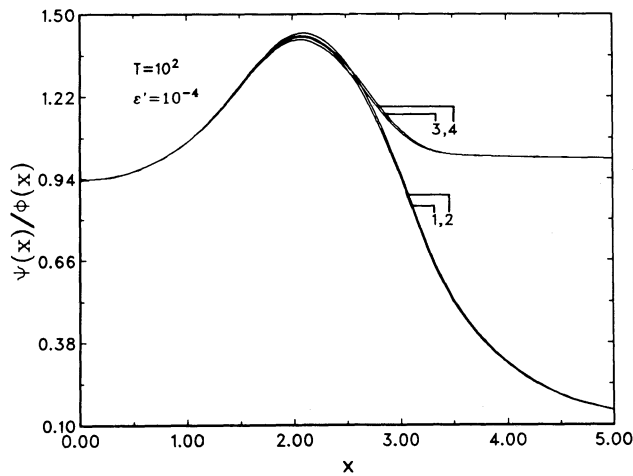


Fig. 4. Same as in Fig. 3 but $\epsilon'=10^{-4}$

3.1. Ratio of the emission profile to the absorption profile

3.1.1. Effectively thin medium

Figure 3 shows $\psi(x)/\phi(x)$ at $\tau=0$ for a self-emitting slab (i.e. no incident radiation) with $T=10^2$ and $\epsilon'=10^{-3}$. From this figure, we see that the R_{II} redistribution gives $\psi(x)/\phi(x)$ nearly equal to 1 for $|x|<1$ but different from 1 at all other frequencies. If we had used the CRD source function we would have obtained the above ratio to be 1 at all the frequencies. From the same figure we see that R_{III} gives $\psi(x) \simeq \phi(x)$ in the above mentioned region and also in the wings. These characteristics are probably due to the fact that these redistribution functions differ from the CRD (see Figs. 1 and 2). The curves show a similar behaviour as those for cases 1 and 2 in Fig. 6.8 obtained by Oxenius (1986). We cannot make an exact comparison because the redistribution function and the thermalization parameter considered by us are quite different. We could reproduce the curves given by Oxenius if we used the Doppler redistribution. When the contribution from the thermal sources is reduced (i.e. ϵ' is reduced to 10^{-4}), we find $\psi(x)/\phi(x)$ follows the same trend (Fig. 4). But the emergent intensity is reduced by an order of magnitude (see Figs. 9 and 10). The emergent intensity is plotted at $\mu=0.78$ in all our figures.

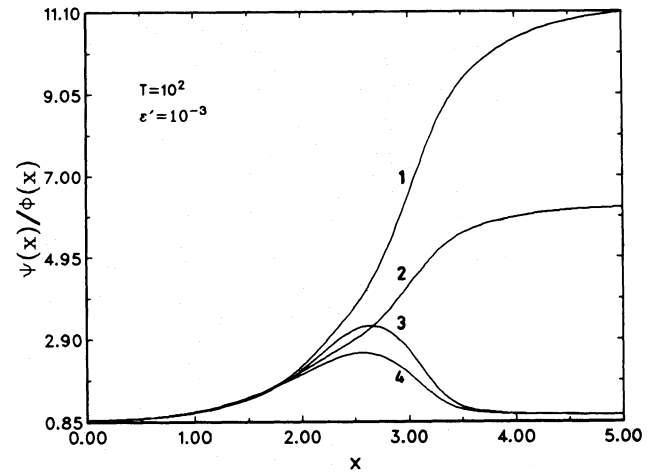


Fig. 5. Same as in Fig. 3 with incident radiation on one of the boundaries

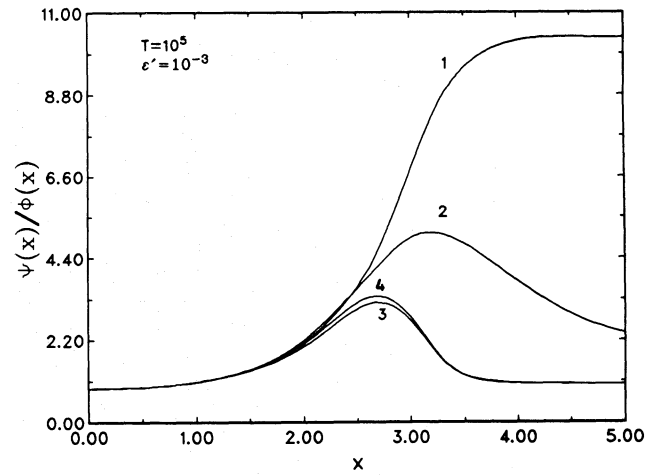


Fig. 6. Same as in Fig. 3 but $T=10^5$

Stimulated emission modifies the optical depth in the spectral line (see the ρ parameter in Eq. 14) and the source function (Eq. 8). Hence it affects the emission profile. Though there is some deviation in the wings for a spectral line formed with stimulated emission, the effect is negligible in the core (see Figs. 9 and 10). Since the radiation transmitted in the wings is so small, we find that the ratio $\psi(x)/\phi(x)$ drops considerably.

When there is incident radiation on one of the boundaries, it is transmitted through the wings for an optically thin medium reaching the incident intensity value of 1 (Fig. 11). Since $R_{II}(x', x)/\phi(x')\phi(x)$ in the wings is nearly 10^3 , we find the emission profile to clearly dominate over the absorption profile (Fig. 5).

3.1.2. Effectively thick medium

An effectively thick medium ($T=10^5$, $\epsilon'=10^{-3}$) emits more radiation (Figs. 12 and 13) compared to an effectively thin medium for a self-emitting slab. Therefore we find the ratio of the emission profile to the absorption profile (Figs. 6 and 7) is

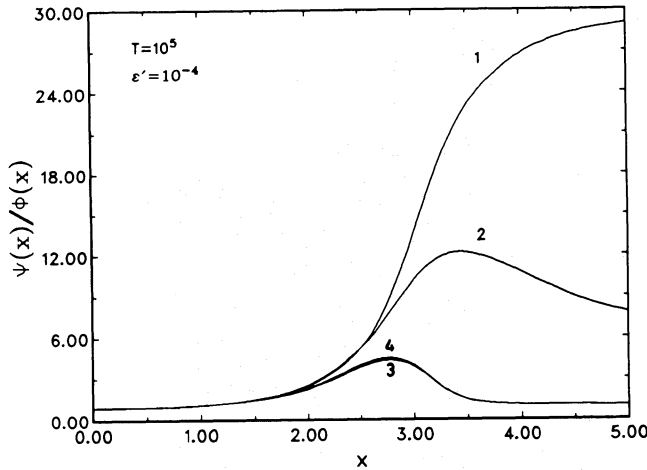


Fig. 7. Same as in Fig. 6 but $\epsilon' = 10^{-4}$

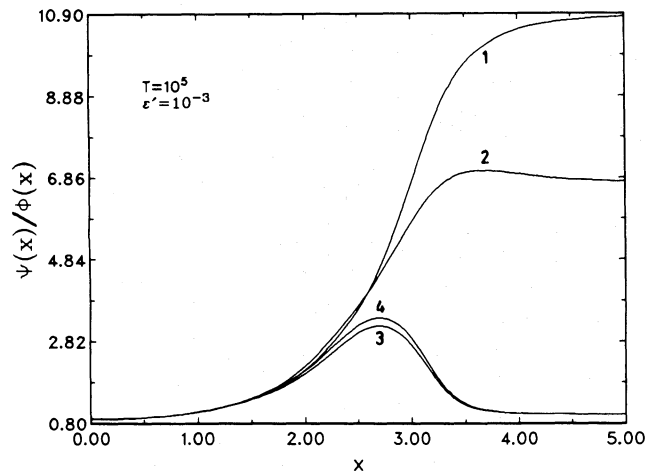


Fig. 8. Same as in Fig. 6 with incident radiation on one of the boundaries

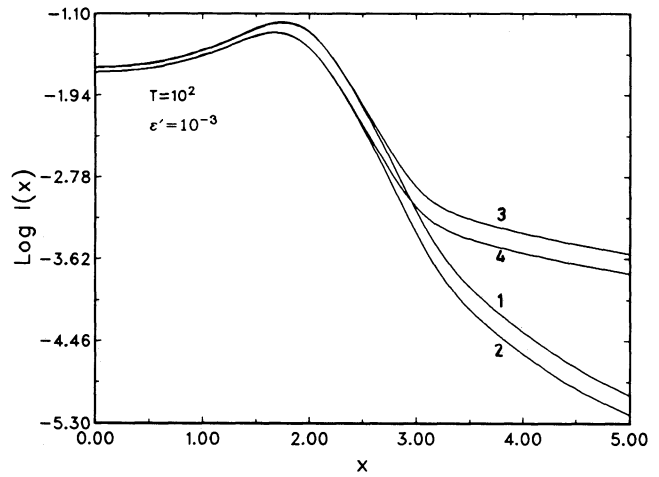


Fig. 9. Emergent intensity is plotted against frequency x , expressed in Doppler units for a self-emitting slab with total optical depth $T=10^2$ and $\epsilon' = 10^{-3}$

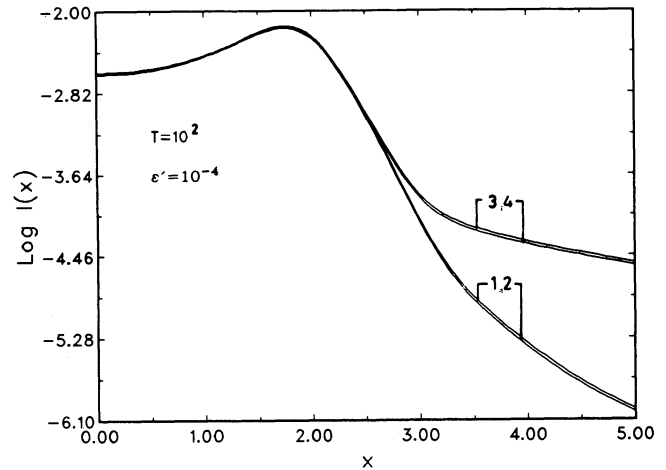


Fig. 10. Same as in Fig. 9 but $\epsilon' = 10^{-4}$

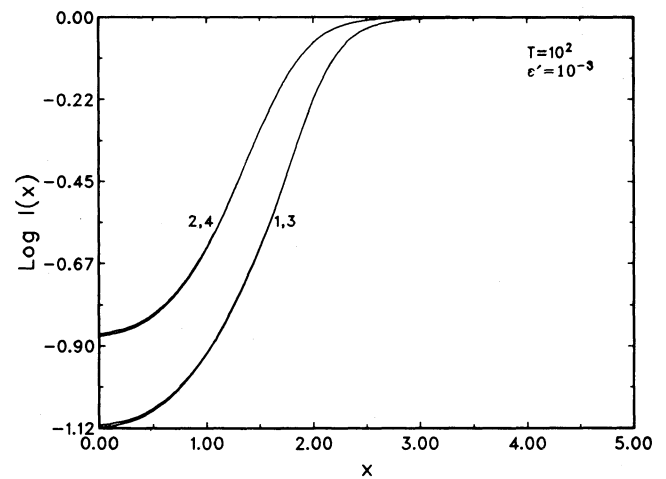


Fig. 11. Same as in Fig. 9 with incident radiation on one of the boundaries

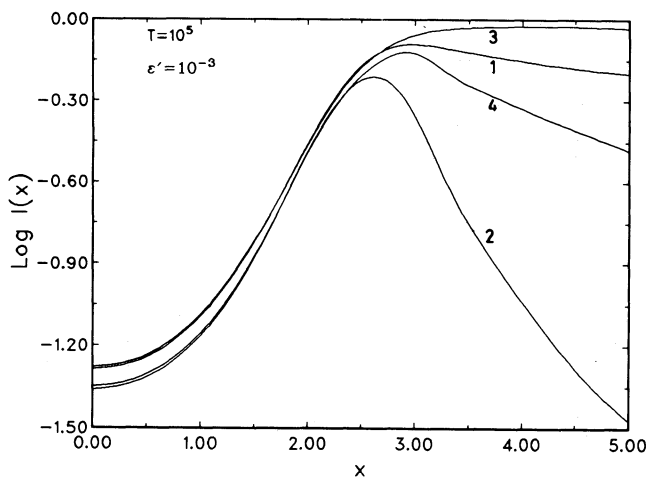


Fig. 12. Same as in Fig. 9 but $T=10^5$

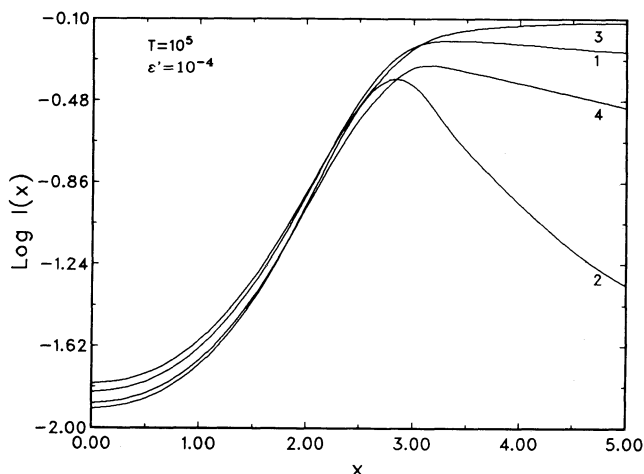


Fig. 13. Same as in Fig. 12 but $\epsilon' = 10^{-4}$

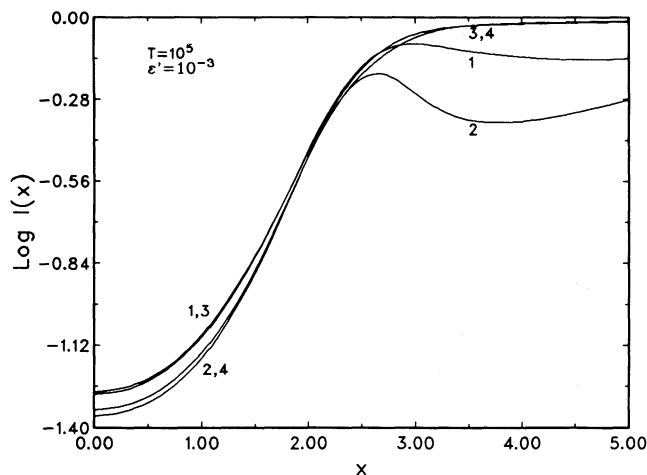


Fig. 14. Same as in Fig. 12 with incident radiation on one of the boundaries

determined by the radiation field in the medium. Comparing Figs. 6 and 7 we note that as ϵ' is increased, the ratio $\psi(x)/\phi(x)$ decreases. These figures show similar trends as those of curves 3 and 4 in Fig. 6.8 of Oxenius (1986).

Stimulated emission decreases the source function as well as the emission profile in the wings. But the optical depth in the wings increases. These factors cause the intensity in the wings to drop by an order of magnitude (Figs. 12 and 13). When the optical depth of the medium is quite high, we find that the incident radiation on one of the boundaries does not produce any significant effect either on the emergent radiation or on the emission profile (compare Figs. 14 and 8 with Figs. 12 and 6) compared to a medium without incident radiation.

4. Conclusions

The type of redistribution function used in the transfer calculations affect the emergent emission profile in a characteristic way. The R_{III} function gives an emission profile identical to the absorption profile (like CRD) in the core and in the wings but with a small enhancement at the intermediate frequency points. For R_{II} , the emergent emission profile is different from the absorption profile in the wing by several factors. When stimulated emission is present, we find that the ratio of the emission profile to the absorption profile and also the wings of the spectral line profiles to be reduced for the R_{II} redistribution. The above conclusions are quite general and hold good for all cases considered in this study. When thermal sources increase in the medium, the ratio $\psi(x)/\phi(x)$ considerably reduces in the wings for an effectively thick medium.

Acknowledgements. We thank the unknown referees for useful comments and suggestions. We also thank Mr. B.A. Varghese for helping us with the plotting routines.

References

- Abramowitz, M., Stegun, I.: 1974, *Handbook of Mathematical functions*, Dover, New York
- Baschek, B., Mihalas, D., Oxenius, J.: 1981, *Astron. Astrophys.* **97**, 43
- Dirac, P.A.M.: 1958, *The principles of quantum mechanics*, Clarendon press, Oxford
- Grant, I.P., Hunt, G.E.: 1969, *Proc. Roy. Soc. Lond. A.* **313**, 183
- Heasley, J.N., Kneer, F.: 1976, *Astrophys. J.* **203**, 660
- Hubeny, I.: 1981, *Bull. Astron. Instit. Czech.* **32**, 271
- Hummer, D.G.: 1962, *Monthly Notices Roy. Astron. Soc.* **125**, 21
- Mihalas, D.: 1978, *Stellar Atmospheres*, 2nd edn., Freeman, San Francisco
- Milkey, R., Mihalas, D.: 1973, *Astrophys. J.* **185**, 709
- Oxenius, J.: 1965, *J. Quant. Spectros. Radiat. Transfer.* **5**, 771
- Oxenius, J.: 1986, *Kinetic Theory of particles and photons*, Springer, Berlin Heidelberg New York Tokyo
- Peraiah, A.: 1978, *Kodaikanal Obs. Bull. Ser. A.* **2**, 115
- Shine, R., Milkey, R., Mihalas, D.: 1975, *Astrophys. J.* **199**, 724
- Steinitz, R., Shine, R.A.: 1973, *Monthly Notices Roy. Astron. Soc.* **162**, 197